Controlled light-pulse propagation via dynamically induced double photonic band gaps

Ren-Gang Wan,[1] Jun Kou,[1] Shang-Qi Kuang,[1,2] Li Jiang,[1] and Jin-Yue Gao[1,*]

[1]*Key Lab of Coherent Light and Atomic and Molecular Spectroscopy of Ministry of Education, College of Physics, Jilin University, Changchun 130023, China*
[2]*Changchun Institute of Optics, Fine Mechanics and Physics, Chinese Academy of Sciences, Changchun 130033. China*
**jygao@mail.jlu.edu.cn*

Abstract: We analyze the optical response of a standing-wave driven four-level atomic system with double dark resonances. Fully developed double photonic band gaps arise as a result of periodically modulated refractive index within the two electromagnetically induced transparency widows. We anticipate that the dynamically induced band gaps can be used to coherently control the propagation of light-pulses with different center frequencies and may have applications in all-optical switching and routing for quantum information networks.

OCIS codes: (270.0270) Quantum optics; (270.1670) Coherent optical effects; (160.5293) Photonic bandgap material.

References and links

1. S. E. Harris, "Electromagnetically induced transparency," Phys. Today **50**(7), 36 (1997).
2. M. Fleischhauer, A. Imamoglu, and J. P. Marangos, "Electromagnetically induced transparency: Optics in coherent media," Rev. Mod. Phys. **77**(2), 633–673 (2005).
3. L. V. Hau, S. E. Harris, Z. Dutton, and C. H. Behroozi, "Light speed reduction to 17 meters per second in an ultracold atomic gas," Nature **397**(6720), 594–598 (1999).
4. M. M. Kash, V. A. Sautenkov, A. S. Zibrov, L. Hollberg, G. R. Welch, M. D. Lukin, Y. Rostovtsev, E. S. Fry, and M. O. Scully, "Ultraslow group velocity and enhanced nonlinear optical effects in a coherently driven hot atomic gas," Phys. Rev. Lett. **82**(26), 5229–5232 (1999).
5. M. Fleischhauer, and M. D. Lukin, "Dark-state polaritons in electromagnetically induced transparency," Phys. Rev. Lett. **84**(22), 5094–5097 (2000).
6. S. E. Harris, and L. V. Hau, "Nonlinear optics at low light levels," Phys. Rev. Lett. **82**(23), 4611–4614 (1999).
7. M. Artoni, and G. C. La Rocca, "Optically tunable photonic stop bands in homogeneous absorbing media," Phys. Rev. Lett. **96**(7), 073905 (2006).
8. Q. Y. He, J. H. Wu, T.-J. Wang, and J.-Y. Gao, "Dynamic control of the photonic stop bands formed by a standing wave in inhomogeneous broadening solids," Phys. Rev. A **73**(5), 053813 (2006).
9. J. H. Wu, G. C. La Rocca, and M. Artoni, "Controlled light-pulse propagation in driven color centers in diamond," Phys. Rev. B **77**(11), 113106 (2008).
10. M. Bajcsy, A. S. Zibrov, and M. D. Lukin, "Stationary pulses of light in an atomic medium," Nature **426**(6967), 638–641 (2003).
11. A. André, M. Bajcsy, A. S. Zibrov, and M. D. Lukin, "Nonlinear optics with stationary pulses of light," Phys. Rev. Lett. **94**(6), 063902 (2005).
12. I. Friedler, G. Kurizki, and D. Petrosyan, "Deterministic quantum logic with photons via optically induced photonic bandgaps," Phys. Rev. A **71**(2), 023803 (2005).
13. J. H. Wu, M. Artoni, and G. C. La Rocca, "All-optical light confinement in dynamic cavities in cold atoms," Phys. Rev. Lett. **103**(13), 133601 (2009).
14. P. S. J. Russell, "Photonic-Crystal Fibers," J. Lightwave Technol. **24**(12), 4729–4749 (2006).
15. C. L. Cui, J. H. Wu, J. W. Gao, Y. Zhang, and N. Ba, "Double photonic bandgaps dynamically induced in a tripod system of cold atoms," Opt. Express **18**(5), 4538–4546 (2010).
16. M. D. Lukin, S. F. Yelin, M. Fleischhauer, and M. O. Scully, "Quantum interference effects induced by interacting dark resonances," Phys. Rev. A **60**(4), 3225–3228 (1999).
17. Y. C. Chen, Y. A. Liao, H. Y. Chiu, J. J. Su, and I. A. Yu, "Observation of the quantum interference phenomenon induced by interacting dark resonances," Phys. Rev. A **64**(5), 053806 (2001).
18. S. F. Yelin, V. A. Sautenkov, M. M. Kash, G. R. Welch, and M. D. Lukin, "Nonlinear optics via double dark resonances," Phys. Rev. A **68**(6), 063801 (2003).
19. Y. P. Niu, S. Q. Gong, R. X. Li, Z. Z. Xu, and X. Y. Liang, "Giant Kerr nonlinearity induced by interacting dark resonances," Opt. Lett. **30**(24), 3371–3373 (2005).

#126707 - $15.00 USD Received 8 Apr 2010; revised 4 Jun 2010; accepted 16 Jun 2010; published 8 Jul 2010

20. C. P. Liu, and S. Q. Gong, "D. C. Cheng, X. J. Fan, and Z. Z. Xu, "Atom localization via interference of dark resonances," Phys. Rev. A **73**, 025801 (2006).

1. Introduction

The phenomenon of electromagnetically induced transparency (EIT) [1,2], which based on the laser induced atomic coherence, plays an important role in the interaction between light and matter and has found numerous applications in light propagation control [3,4], light storage [5], enhancement of nonlinearity at low light levels [6], etc. The usual EIT-scheme is three-level Λ system driven by a strong traveling-wave (TW) coupling field. Yet, when the coupling field has a standing-wave (SW) pattern, the optical response of the probe is modulated periodically in the space. This has been explored to obtain photonic band gap (PBG) [7–9], to generate stationary light pulse [10], to enhance optical nonlinearity [11], to realize deterministic quantum logic [12], and to devise optical cavity [13], etc. Most recently, multiple PBGs are obtained in some systems, such as photonic-crystal fibers [14] and multi-standing-wave driven atoms [15].

It is well know that basis of EIT is the existence of dark resonance. As the single dark state is coherently coupled to another level by a control field, double dark resonances arise and the atom exhibits two EIT windows [16,17]. The interferences between the dark resonances allow us to well manipulate the optical responses of atoms [18–20]. Inspired by these studies, we here demonstrate a coherent control of light-pulse propagation via induced double PBGs in a SW driven double-dark-resonance system. Due to the spatial modulation of probe refractive index, a pair of PBGs open up in the two EIT regions and can be tuned dynamically. The double-dark-resonance scheme has more degree of freedom in manipulating light-pulse than the single-dark-resonance scheme with only one PBG.

2. Theoretical model

Consider the four-level system in cold ^{87}Rb atoms shown in Fig. 1. The levels $|1\rangle$, $|2\rangle$, $|3\rangle$ and $|4\rangle$ may correspond to the hyperfine states $|5P_{3/2}, F=2, m_F=1\rangle$, $|5S_{1/2}, F=2, m_F=0\rangle$, $|5S_{1/2}, F=2, m_F=2\rangle$ and $|5S_{1/2}, F=1, m_F=0\rangle$. A strong SW coupling field with space-dependent Rabi frequency $\Omega_c(z)$ couples levels $|2\rangle$ and $|3\rangle$, a weak probe field Ω_p couples levels $|1\rangle$ and $|2\rangle$, and a microwave control field Ω_d drives levels $|3\rangle$ and $|4\rangle$. In real experiments, the coupling and probe fields are circularly polarized with right and left helicities, and propagate along the z axis defined by a static magnetic field, while the control field is linearly polarized with polarization direction close to the z axis.

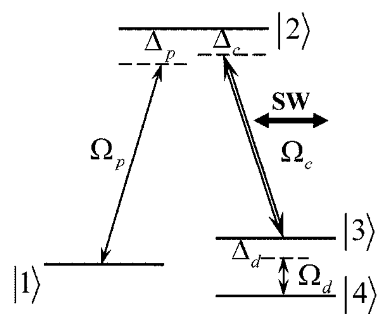

Fig. 1. Four-level atomic system with double dark resonances.

To deal with the optical properties of such a SW driven system, we start with its steady response. By solving the density-matrix equations under weak field approximation, the linear susceptibility χ_p and the refractive index n_p experienced by the probe are derived as

$$\chi_p(\Delta_p, z) = 3\pi\mathcal{N}\,\frac{\gamma_{21}(\Gamma_{31}\Gamma_{41} - \Omega_d^2)}{\Gamma_{21}(\Gamma_{31}\Gamma_{41} - \Omega_d^2) - \Gamma_{41}\Omega_c^2(z)},$$
$$n_p(\Delta_p, z) = \sqrt{1+\chi_p(\Delta_p, z)}, \tag{1}$$

where $\mathcal{N} = N_0(\lambda_p/2\pi)^3$, N_0 is the atomic density. $\Gamma_{21} = \Delta_p - i\gamma_{21}$, $\Gamma_3 = \Delta_p - \Delta_c - i\gamma_{31}$, and $\Gamma_4 = \Delta_p - \Delta_c - \Delta_d - i\gamma_{41}$, with γ_{ij} being the dephasing rate of the respective atomic coherence ρ_{ij}, and $\Delta_p = \omega_{21} - \omega_p$, $\Delta_c = \omega_{23} - \omega_c$, and $\Delta_p = \omega_{21} - \omega_p$ are the detunings of the three fields from the corresponding transitions.

Unlike in typical double-dark-resonance system where a TW coupling field is used, the coupling here has a SW pattern which generated from the retroreflection on a mirror of reflectivity R_m. Then the resulting squared coupling Rabi frequency varies periodically along z as

$$\Omega_c^2(z) = \Omega_0^2[(1+\sqrt{R_m})^2\cos^2(k_c z) + (1-\sqrt{R_m})^2\sin^2(k_c z)], \tag{2}$$

where k_c is the wave vector of the coupling field. It is clear that $\Omega_c^2(z)$ has a spatial periodicity of $a = \lambda_c/2$, which may be changed into $a = \lambda_c/[2\cos(\theta/2)]$ via slightly misaligning the forward and backward coupling fields by an angle θ. Clearly, the complex refractive index $n_p(\Delta_p, z)$ also varies periodically in the z direction. With $n_p(\Delta_p, z)$ in hand, we further obtain the 2×2 unimodular transfer matrix $M(\Delta_p)$ describing the probe propagation through a single period of length a. The translational invariance of the periodic medium requires that the Bloch condition must be imposed on the photonic eigenstates, i.e

$$\begin{pmatrix} E^+(x+a) \\ E^-(x+a) \end{pmatrix} = M(\Delta_p)\begin{pmatrix} E^+(x) \\ E^-(x) \end{pmatrix} = \begin{pmatrix} e^{i\kappa a}E^+(x) \\ e^{i\kappa a}E^-(x) \end{pmatrix}, \tag{3}$$

where E^+ and E^- are the amplitudes of the forward and backward electric field of the probe. $\kappa = \kappa' + i\kappa''$ is the complex Bloch wave vector, which represents the photonic band gap structure, and can be obtained from solutions of the equation $e^{2i\kappa a} - \mathrm{Tr}[M(\Delta_p)]e^{i\kappa a} + 1 = 0$ [7]. For a sample of length $l = Na$ with N being the number of the SW periods, the total transfer matrix can be expressed as $M_N = M^N$, and the reflection and transmission amplitudes for the probe are given by

$$r(\Delta_P) = \frac{M_{N(12)}(\Delta_P)}{M_{N(22)}(\Delta_P)} = \frac{M_{12}\sin(N\kappa a)}{M_{22}\sin(N\kappa a) - \sin[(N-1)\kappa a]},$$
$$t(\Delta_P) = \frac{1}{M_{N(22)}(\Delta_P)} = \frac{\sin(\kappa a)}{M_{22}\sin(N\kappa a) - \sin[(N-1)\kappa a]}, \tag{4}$$

with $M_{N(ij)}$ being the matrix elements of M_N. Then the reflectivity $R(\Delta_P) = |r(\Delta_P)|^2$ and the transmissivity $T(\Delta_P) = |t(\Delta_P)|^2$ can be calculated easily.

By utilizing Eq. (4) and the Fourier transform method [9], we can further study the propagation dynamics of an incident probe pulse. Here, we assume that the input probe has Gaussian profiles in the time and frequency domains as

#126707 - $15.00 USD Received 8 Apr 2010; revised 4 Jun 2010; accepted 16 Jun 2010; published 8 Jul 2010

$$E_{It}(t)=E_{0t}e^{-(t-t_0)^2/\delta_t^2},$$
$$E_{If}(\Delta_p)=E_{0f}e^{-(\Delta_p-\Delta_{p0})^2/\delta_p^2}, \quad (5)$$

where $E_{0f}=\sqrt{\pi}\delta_t E_{0t}$, $\delta_p=2/\delta_t$, t_0 and δ_t (Δ_{p0} and δ_p) are the center and width of the input probe pulse in the time (frequency) domain. Then we obtain the reflected and the transmitted Fourier components from $E_{Rf}(\Delta_p)=E_{If}(\Delta_p)\cdot r(\Delta_p)$ and $E_{Tf}(\Delta_p)=E_{If}(\Delta_p)\cdot t(\Delta_p)$, so that the reflected and transmitted probe pulse in the time domain can be derived via inverse Fourier transform, given by

$$E_{Rt}(\Delta_p)=\int E_{Rf}(\Delta_p)e^{i(\Delta_p-\Delta_{p0})t}d(\Delta_p),$$
$$E_{Tt}(\Delta_p)=\int E_{Tf}(\Delta_p)e^{i(\Delta_p-\Delta_{p0})t}d(\Delta_p). \quad (6)$$

3. Numerical results

As pointed out by Lukin *et al.* [16], the coherent interaction between the single dark state and the control field Ω_d leads to the emergence of double dark resonances at the frequencies $\Delta_\pm=(2\Delta_c+\Delta_d\pm\sqrt{\Delta_d^2+4\Omega_d^2})/2$, which indicate two distinct EIT windows for the probe. In the present scheme, as a result of the SW coupling field, the probe absorption and dispersion are modified along z axis with the same periodicity as the SW. Therefore, the probe field propagates as in a one-dimensional multilayer periodic structure which has two transparent regions determined by the double EIT. Consequently, double PBGs are expected to occur at Brillouin zone boundary π/a.

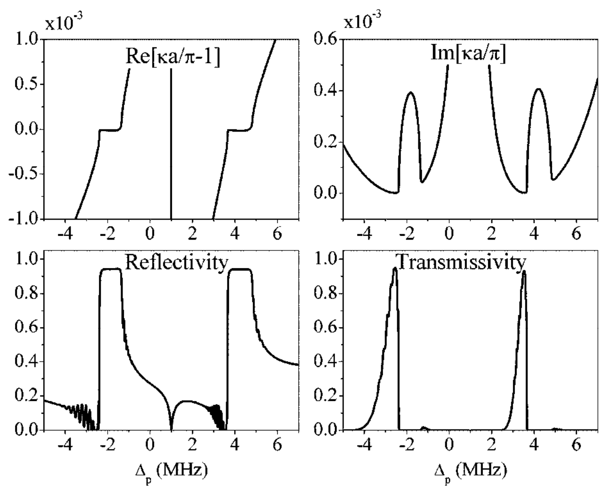

Fig. 2. Band gap structure near the first Brillouin zone boundary in terms of Bloch wave vector, and the probe reflectivity and transmissivity spectra for a 1.0 cm long atomic sample. Parameters are $N_0=1.0\times10^{12}cm^{-3}$, $\eta=0.12$, $\theta=20mrad$, $\gamma_{21}=6MHz$, $\gamma_{31}=\gamma_{41}=1KHz$, $\Omega_0=40MHz$, $\Omega_d=3MHz$, $\Delta_c=0$, and $\Delta_d=1MHz$.

Figure 2 shows the PBGs structure in terms of the Bloch wave vector and the reflection and transmission spectra. First of all, it is worth mentioning that an imperfect SW coupling with unequal forward and backward components is applied so that double EIT are established everywhere, even at nodes of the SW. Therefore, the probe experiences no absorption and the band gaps can be well developed. We here define a parameter $\eta=(1-\sqrt{R_m})/(1+\sqrt{R_m})$ to

#126707 - $15.00 USD Received 8 Apr 2010; revised 4 Jun 2010; accepted 16 Jun 2010; published 8 Jul 2010

describe the degree of imperfectness of the SW. As can be seen in Fig. 2, a pair of PBGs open up in the frequency ranges where $\kappa' = \pi/a$ and $\kappa'' \neq 0$. Within the gaps, $\kappa'' \neq 0$ corresponds to reflection rather than absorption and the probe reflectivity is nearly 95%. On the left of the band edges, there are two narrow regions with high transmissivity (95% at maximum) for the probe, and the positions of the two left band edges are determined by the dark resonances which occur at $\Delta_p = \Delta_{\pm}$. Therefore, we can tune the gap positions by changing $\Delta_{\pm}$. Figure 3 displays the variation of the band-gap structure for different control Rabi frequencies. Moreover, the detunings Δ_c and Δ_d, and the coupling Rabi frequency Ω_0 can also be applied to tuning the positions and widths of the gaps.

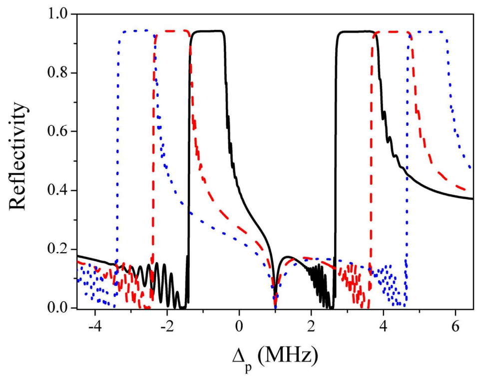

Fig. 3. (Color online) Tuning of the band-gap reflectivity for different control intensities with $\Omega_d = 2MHz$ (black-solid), $\Omega_d = 3MHz$ (red-dashed), and $\Omega_d = 4MHz$ (blue-dotted). Other parameters are the same as in Fig. 2.

The coherently induced double PBGs allow us control the light-pulse propagation all-optically. Consider an incident Gaussian pulse of which the amplitude of electric field can be written as $E_{It}(t) = E_{0t} e^{-(t-t_0)^2/\delta_t^2}$ and the central probe detuning is denoted by Δ_{p0}, Fig. 4 shows the reflected part at $z = 0$ (red-dashed) and transmitted part at $z = l$ (blue-dotted). It is obviously that the dynamics of light-pulse propagation are sensitive to the central detuning Δ_{p0} of the incident probe. If most of the carrier frequencies of the probe are inside the band gaps ($\Delta_{p0} = -2.0MHz$ and $\Delta_{p0} = 4.0MHz$), the pulse is reflected with little attenuation or distortion except a short time delay [Fig. 4(c) and Fig. 4(f)]. As the center frequencies of the probe move near the band edge ($\Delta_{p0} = -2.4MHz$ and $\Delta_{p0} = 3.65MHz$), i.e. only partial carrier frequencies fall into the PBGs, the reflected part is increasingly suppressed and distorted, while a stronger transmitted part is observed [Fig. 4(b) and Fig. 4(e)]. Both parts are broadened due to the decrease of carrier-frequency components, and the latter experiences slow-light propagation as a result of strong EIT dispersion. If most of the carrier frequencies lie inside the transmission regions ($\Delta_{p0} = -2.6MHz$ and $\Delta_{p0} = 3.5MHz$), the probe pulse transmits subluminally through the atoms with a large time delay [Fig. 4(a) and Fig. 4(d)]. The loss and broadening of the pulse is owing to the narrow transmission and group-velocity dispersion.

The double PBGs scheme is more appealing than the single PBG scheme in real applications, because it can synchronously manipulate two weak light signals with distinct frequencies. For two pulses, by turning on the SW (double PBGs) or the TW (double EIT windows) coupling, we can either let them be reflected or be transmitted with little attenuation and deformation. This can be applied to all-optical switching or routing with two channels.

#126707 - $15.00 USD Received 8 Apr 2010; revised 4 Jun 2010; accepted 16 Jun 2010; published 8 Jul 2010

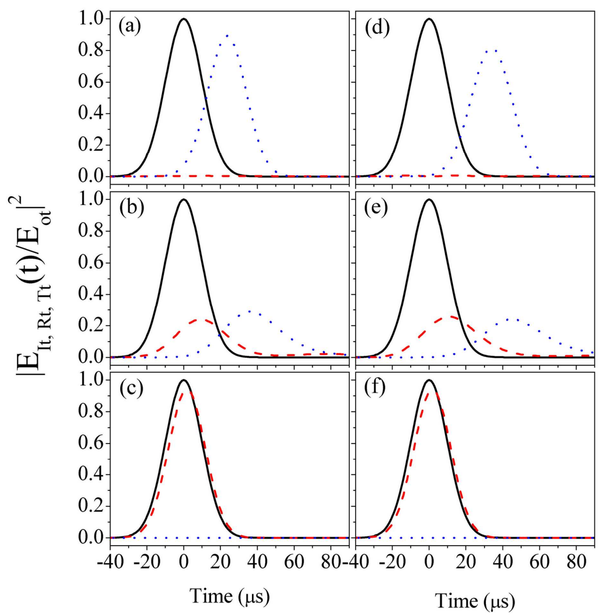

Fig. 4. (Color online) Pulse dynamics of an incident (black-solid) probe impinging upon a long sample with the reflected (red-dashed) and transmitted (blue-dotted) parts shown. The frequency widths and centers of the incident pulsed are $\delta_t = 20\mu s$, $t_0 = 0$ and (a) $\Delta_{p0} = -2.6MHz$, (b) $\Delta_{p0} = -2.4MHz$, (c) $\Delta_{p0} = -2.0MHz$, (d) $\Delta_{p0} = 3.5MHz$, (e) $\Delta_{p0} = 3.65MHz$, (f) $\Delta_{p0} = 4.0MHz$. Other parameters are the same as in Fig. 2.

4. Conclusion

In conclusion, the optical response of a double-dark-resonance atomic system driven by a SW is investigated. The results show that fully developed double PBGs open up in the two EIT windows as a result of the periodically modulated refractive index, and the band-gap structure can be coherently controlled via tuning the positions and widths of the dark resonances. Moreover, the dynamically induced double PBGs provide an avenue to manipulate the light-pulse propagation. Such a double stop-bands mechanism can easily be exploited to implement a double-channel all-optical switching or routing for simultaneous information processing of two weak light-pulses with different central frequencies. We expect that it may have applications in optical network and quantum information processing.

Acknowledgements

The authors would like to thank the financial supports from NSFC (Grant No. 10774059), and the National Basic Research Program (Grant No. 2006CB921103) of P. R. China.